Influence of a nonionic surfactant on curcumin delivery of nanocellulose reinforced chitosan hydrogel

Influence of a nonionic surfactant on curcumin delivery of nanocellulose reinforced chitosan hydrogel

Article

Accepted Version

Influence of a nonionic surfactant on curcumin delivery of nanocellulose reinforced chitosan hydrogel

Thennakoon M. Sampath Udeni Gunathilake[a], Yern Chee Ching[a], Cheng Hock Chuah[b], Hazlee Azil Illias[c] Kuan Yong Ching[d], Ramesh Singh[e], Liou Nai-Shang[f]

[a]Department of Chemical Engineering, Faculty of Engineering, University of Malaya, 50603 Kuala Lumpur, Malaysiab
[b]Department of Chemistry, Faculty of Science, University of Malaya, 50603 Kuala Lumpur, Malaysia
[c]University of Reading Malaysia, Persiaran Graduan, Kota Ilmu, Educity, 79200 Iskandar Puteri, Johor, Malaysia
[d]Department of Electrical Engineering, Faculty of Engineering, University of Malaya, 50603 Kuala Lumpur, Malaysia
[e]Department of Mechanical Engineering, Faculty of Engineering, University of Malaya, 50603 Kuala Lumpur, Malaysia
[f]Department of Mechanical Engineering, Southern Taiwan University of Science and Technology, 710 Tainan City, Taiwan, ROC

Abstract

Nanocellulose reinforced chitosan hydrogel was synthesized using chemical crosslinking method for the delivery of curcumin which is a poorly water-soluble drug. Curcumin extracted from the dried rhizomes of *Curcuma longa* was incorporated to the hydrogel via in situ loading method. A nonionic surfactant (Tween 20) was incorporated into the hydrogel to improve the solubility of curcumin. After the gas foaming process, hydrogel showed large interconnected pore structures. The release studies in gastric medium showed that the cumulative release of curcumin increased from 0.21% ± 0.02% to 54.85% ± 0.77% with the increasing of Tween 20 concentration from 0% to 30% (w/v) after 7.5 h. However, the entrapment efficiency percentage decreased with the addition of Tween 20. The gas foamed hydrogel showed higher initial burst release within the first 120 minutes compared to hydrogel formed at atmospheric condition. The solubility of curcumin would increase to 3.014 ± 0.041 mg/mL when the Tween 20 concentration increased to 3.2% (w/v) in simulated gastric medium. UV-visible spectra revealed that the drug retained its chemical activity after in vitro release. From these findings, it is believed that the nonionic

surfactant incorporated chitosan/nanocellulose hydrogel can provide a platform to overcome current problems associated with curcumin delivery.

Key words: Nanocellulose, chitosan, hydrogel, curcumin, Tween 20

1. Introduction

Curcumin is a lipophilic polyphenol compound which is derived from rhizomes of *Curcuma longa. Curcumin* is usually a mixture of three curcuminoids (curcumin, demethocycurcumin, and bisdemethoxycurcumin) and volatile oil [1]. Among all former studies on antibacterial activity of curcumin, the most promising result showed is its effectiveness in against *Helicobacter pylori* [2]. *H. pylori* is a microaerophilic bacterium which lives in the sticky mucus that lines the stomach and it has attracted great attention as a main cause of peptic ulcer disease. International agency for research on cancer has defined *H. pylori* as a group I carcinogenic agent of human gastric cancer [3]. Recent studies on the inhibition of *H. pylori* using curcumin by Mahady, Pendland, Yun and Lu [4] showed that both of the curcumin and methanolic extract of turmeric rhizome has inhibited the growth of 19 different strains of *H. pylori.* Furthermore, De, Kundu, Swarnakar, Ramamurthy, Chowdhury, Nair and Mukhopadhyay [3] mentioned that the minimum inhibitory concentration of curcumin for 23% strains of *H. pylori* was about 10 μg/mL and for 58% strains, it was 15 μg/mL. Sometimes antibiotics are likely to be associated with adverse side effects on the host such as allergic reactions, hypersensitivity and immune-suppression. Therefore, there is an increasing demand to develop an alternative antimicrobial drugs using medicinal plants for the treatments of infectious diseases [5].

Although curcumin exerts various biological effects, its limited aqueous solubility and rapid presystemic metabolism has restricted its bioavailability**.** Therefore, the advanced drug delivery systems like nanoparticles, liposomes, micellar formulations, cyclodextrin inclusion complexes, microemulsions and different hydrogel based delivery systems have been developed to circumvent their bioavailability issues [6-8]. Due to the variations on pH along the gastrointestinal tract, the stimuli responsive (e.g.: pH sensitive) hydrogels have been used to deliver various types of drugs to the different locations of the gastro intestinal tract [6-8]. In this study, nanocellulose reinforced chitosan hydrogel was used as a carrier for drug delivery of curcumin. From our previous study [9-11], we observed an improvement of mechanical properties of the biopolymer based composite and hydrogel with physical reinforcement of nanocellulose into the biopolymer matrix. Further, it showed that the swelling characteristics of the hydrogel has improved with the addition of low concentrations of nanocellulose. The system has also exerted the highest swelling properties in acidic medium [10]. It is also observed that the chitosan hydrogel reinforced with 0.5% CNC has successfully achieved the highest swelling properties and cumulative release of curcumin [8,10]. Therefore, in this study, 0.5% CNC-chitosan hydrogel formulation was selected for further improvement of drug delivery properties of the hydrogel. Previous results [8,10] also showed that the percentage of curcumin encapsulation and the amount of curcumin release increased in the gas foam hydrogel (due to the formation of large interconnected pore structures). However, poor solubility of curcumin has caused less concentrations of released drug in simulated gastric medium [8]. Therefore, a nonionic surfactant (Tween 20) has been incorporated into the hydrogel as a solubilizing agent for curcumin in this study.

Surfactants can improve the solubility of some poorly soluble drugs. Tween surfactants contain hydrophilic ethylene glycol head and a hydrophobic alkyl chain [12]. The commonly used Tween are Tween 20, 40, 60 and 80. They possess same hydrophilic group with different length of alkyl chains. The alkyl chain length will influence the hydrophile–lipophile balance (HLB) value of the surfactant, which in turn directly influences the entrapment efficiency of the drug [13]. Low HLB value corresponds to high hydrophobicity. Higher HLB value indicates the more water soluble the surfactant [14]. Tween 20 with HLB value of 16.7 is more hydrophilic in nature compared to other Tween surfactants [15]. Ratanajiajaroen, Watthanaphanit, Tamura, Tokura and Rujiravanit [16] reported that the addition of 2% (v/v) of Tween 20 has increased the solubility of curcumin from 11 ng/mL to 0.767 mg/mL in acetate buffer (pH 5.5). In addition, they obtained higher release rate of curcumin from chitin beads as the amount of Tween 20 increased. O'Toole, Henderson, Soucy, Fasciotto, Hoblitzell, Keynton, Ehringer and Gobin [17] observed that the curcumin can be released completely from the submicrometer spray-dried chitosan/Tween 20 particles in both 1% acetic acid and phosphate buffered saline solutions over a 2 h period. Furthermore, the research works by Petchsomrit, Sermkaew and Wiwattanapatapee [18] also reported that the percentage of curcumin release increased with increasing the Tween 80 concentration in oil entrapped alginate beads. Their results showed that the cumulative drug release increased up to 70% with the incorporation of 25% (w/v) of Tween 80.

Previous cytotoxicity studies revealed that nonionic surfactant such as Tween has lower toxic effect than cationic, anionic and amphoteric ones [19]. Due to its less cytotoxicity properties, the nonionic surfactant was selected for this study. Besides that, surfactants have a profound effect on the release rate of the drug from the encapsulated matrix. Using proper concentration of surfactant and a suitable HLB value, the cumulative release and rate of release of the drug can be

controlled. According to the previous studies, the surfactants with lower HLB values such as Tween 80 would cause lower release rates of hydrophobic drugs. This is because the surfactants having lower HLB values are more lipophilic and less water soluble. But with higher HLB values, hydrophobic drug release rate will increase as these surfactants are more hydrophilic and water soluble [20]. Tween 20 has a high HLB value of 16.7 and this will help to improve the release of hydrophobic drug to a desired level. Tween 80 had been successfully applied in many hydrophobic drug delivery systems [21-25]. However, the investigations on polysorbate-chitosan association by Picone and Cunha [26] has shown that the longer hydrophobic polysorbate tail length of Tween 80 has made it difficult to form homogeneous association with chitosan. Their further investigations had found that the shorter hydrophobic tail length of Tween 20 was more appropriated to form mixed surfactant–chitosan polymer systems. So, Tween 20 which is a less cytotoxic, nonionic, with shorter hydrophobic tail length surfactant was used to improve the drug release of curcumin from nanocellulose reinforced chitosan hydrogel matrix in this study.

The objective of this study was to improve the bioavailability of less water-soluble curcumin by incorporating a nonionic surfactant (Tween 20) to nanocellulose reinforced chitosan hydrogel. Curcumin extracted from dried rhizomes of *Curcuma longa* and Tween 20 was incorporated to the hydrogel via in situ loading method. From our previous study, a large extent of chitosan matrix swelling was found to occur in acidic medium [10]. Therefore, the drug molecules are expected to diffuse extensively through the swollen gel into the exterior medium at gastric pH levels. Nonionic surfactant will further facilitate dissolution of the drug by partitioning the drug into the aqueous phase of gastric fluid. Based on the results of this study, it is expected that the nanocellulose reinforced chitosan hydrogel/Tween 20 drug delivery system will provide a

platform to overcome poor bioavailability of curcumin to yield its broad range of therapeutic benefits.

2. Materials and Methods

2.1. Materials

Chitosan with medium molecular weight (viscosity 200–500 cP, 0.5% acetic acid at 20 ℃), acetic acid glacial grade AR, sodium chloride, hydrochloric acid, methanol and sulfuric acid were purchased from Friendemann Schmidt Chemicals (Parkwood, Australia). The drug curcumin was provided by HIMEDIA laboratories Pvt Ltd. (Mumbai, India). Glutaraldehyde 25% (for crosslinking of chitosan) was obtained from Thermo Fisher Scientific Inc. (Victoria, Australia). Microcrystalline cellulose, Tween 20 and phosphate-buffered saline were supplied by R&M chemicals (Essex, UK).

2.2. Research Methodology

2.2.1. Extraction of curcumin from turmeric

Curcumin was extracted from rhizomes of *Curcuma longa* following the method proposed elsewhere [5]. Dried rhizomes were crushed in a mortar and pestle. Crushed rhizomes were soaked in methanol for 3 days and then filtered with Whatman filter paper (pore size 0.2 µm). After that, filtrate was poured into a petri plate and the solvent was evaporated under vacuum condition to obtain semi-dry oily mass.

2.2.2. Preparation of curcumin loaded chitosan/nanocellulose/Tween20 hydrogel

Cellulose nanocrystals (CNC) were prepared from microcrystalline cellulose by sulfuric acid hydrolysis method reported in our previous study [10]. Chitosan was dissolved in 5% (v/v)

aqueous acetic acid solution at room temperature and left overnight in the shaker with the rotation rate of 250 rpm and then filtered through the filter paper to remove any insoluble matters. To prepare curcumin loaded chitosan/nanocellulose/Tween 20 hydrogel, nanocellulose, extracted curcumin and Tween 20 were added to chitosan solution and stirred (250 rpm) for one hour. After that glutaraldehyde was added and stirred (350 rpm) for 1 min at room temperature. The mixture was then poured into the mold and the hydrogel was allowed to solidify at room temperature for 24 h.

Formulation	Chitosan (w/v)%	Nanocellulose (w/v)%	Tween 20 (w/v)%	Glutaraldehyde (v/v)%	Curcumin (mg per 2.5 g of hydrogel disc)
CH/CNC/ TW-0%	2	0.5	0	0.2	1.5
CH/CNC/ TW-5%	2	0.5	5	0.2	1.5
CH/CNC/ TW-10%	2	0.5	10	0.2	1.5
CH/CNC/ TW-15%	2	0.5	15	0.2	1.5
CH/CNC/ TW-20%	2	0.5	20	0.2	1.5
CH/CNC/ TW-25%	2	0.5	25	0.2	1.5
CH/CNC/ TW-30%	2	0.5	30	0.2	1.5

Table 1: Composition of curcumin entrapped chitosan/nanocellulose/Tween 20 hydrogel

2.2.3. CO_2 gas foaming of curcumin entrapped chitosan/nanocellulose/Tween 20 hydrogels

After mixing the CNC, drug, Tween 20 and crosslinker with chitosan solution as described above, the mixture was poured into the mold and placed inside the gas foaming apparatus. Then the apparatus was pressurized with CO_2 to predetermined pressure (50 bar). The pressure was maintained to allow for CO_2 saturation and chitosan crosslinking for 48 h. The system was then depressurized at 1 bar/min to result in the generation of numerous gas bubbles which induce gas foaming.

2.3. Characterization

2.3.1. Characterization of curcumin

UV-visible spectra of both curcumin (HIMEDIA Co.) and curcumin extracted from turmeric were obtained by scanning the drug solutions within the range of 350-800 nm using UV-visible spectrophotometer (Shimadzu, Kyoto, Japan). FTIR studies on curcumin purchased from HIMEDIA Co. and curcumin extracted from turmeric, were carried out using PerkinElmer spectrum 400 FTIR spectrometer over the range 3000–500 cm^{-1}.

2.3.2. Characterization of the curcumin entrapped chitosan/nanocellulose/Tween 20 hydrogels

2.3.2.1. FTIR analysis

FTIR studies of raw materials and various composition of hydrogel composites were carried out by using PerkinElmer spectrum 400 FTIR spectrometer over the range 3000–500 cm^{-1}.

2.3.2.2. Morphology Studies

The morphology of the hydrogels was examined using field emission scanning electron microscope (FE-SEM, SU8220). Hydrogels were freeze dried using freeze dryer to remove water without disturbing the morphology. The hydrogels were then coated with platinum in order to prevent the charging effects at an accelerating voltage of 5 kV.

2.4. Drug delivery studies

2.4.1. Estimation procedure of curcumin by UV-Vis spectrophotometer

The absorption maxima (λ_{max}) for curcumin was determined by scanning the drug solution within the range of 350-800 nm using UV-Vis spectrophotometer. It was found that the drug exhibited λ_{max} at 427 nm in both of the distilled water and simulated gastric medium as shown in Fig. 1a and Fig. 2a, respectively. The concentration of curcumin extracted from turmeric was determined by the standard calibration curve (λ_{max} at 427 nm) prepared using standard solutions of curcumin (HIMEDIA Co).

The concentration of curcumin present in distilled water was determined from the calibration curve (Fig. 1b) prepared from standard solutions of curcumin (HIMEDIA Co.), dissolved in methanol and diluted by distilled water.

Fig. 1. a) UV–Vis absorbance spectrum of curcumin in distilled water and b) calibration curve of curcumin.

The concentration of curcumin present in simulated gastric fluid was determined from the calibration curve (Fig. 2b) prepared from standard solutions of curcumin (HIMEDIA Co.), dissolved in methanol and diluted by simulated gastric fluid [27, 28].

Fig. 2. a) UV–Vis absorbance spectrum of curcumin in simulated gastric medium and b) calibration curve of curcumin.

2.4.2. Drug entrapment efficiency

Disc shape hydrogel (1.80 cm diameter and 1.20 cm height) was immersed in 30 mL ethanol for 24 h. Then, the solution was filtered and diluted suitably to measure the absorbance, from which the concentration of drug was calculated using the standard calibration data. Each formulation was analyzed in triplicate and average values were taken. The drug entrapment efficiency was calculated based on the ratio of actual amount of drug present in the hydrogel to the initial amount of drug contained in the hydrogel by using Equation (1).

$$\text{Entrapment efficiency} = \frac{\text{Actual amount of curcumin in hydrogel}}{\text{Initial amount of curcumin contained in the hydrogel}} \quad (1)$$

2.4.3. Drug release

In vitro drug release from hydrogel networks with different Tween 20 concentrations was investigated in simulated gastric fluid (simulated gastric fluid was prepared by dissolving 2 g NaCl in 7.0 mL HCl and water up to 1000 mL) at 37 °C [29]. In order to study the release, 3 mL aliquot was withdrawn at predetermined time intervals and returned it back to the solution after the analysis. The concentration of released curcumin was determined by the calibration curve (Fig. 2b) prepared using the curcumin (HIMEDIA Co.) in simulated gastric fluid. The experiments were performed triplicates and average values were taken.

2.4.4. Drug activity

In drug delivery systems, the chemical and biological activity of drug after release into the body is the most critical parameter. The drug activity of curcumin before loading and after release could be studied by using UV-Vis spectrophotometer [30]. UV- visible spectra of pure drug and the drug released from the hydrogel formed at atmospheric condition were obtained by scanning the solutions within the range of 350-800 nm using UV-visible spectrophotometer. Drug activity was determined through comparison between the spectra (the absorption maxima (λ_{max})) of pure drug and released drug.

2.5. Curcumin solubility studies

To determine a saturated concentration of curcumin in simulated gastric fluid, an excess amount of curcumin (extracted from turmeric) was added in to 30 mL of simulated gastric fluid with different concentrations of Tween 20 (0.8%, 1.6%, 2.4%, 3.2%, 4%, 5.6% (w/v)). Then, the mixtures were stirred (350 rpm) using magnetic stirrer at 37 °C for 12h. Samples were covered to avoid exposition to the light. After that, the solutions were centrifuged at 10,000 rpm for 10 min, supernatant was decanted and the dissolved curcumin was determined using the standard calibration curve prepared using the curcumin (HIMEDIA Co.) in simulated gastric fluid (Fig. 2b).

3. Results and discussion

3.1 Characterization of curcumin

As shown in Fig. 3, the UV-visible spectra of curcumin (HIMEDIA Co.) and curcumin extracted from turmeric were obtained by scanning the drug solutions within the range of 350-800 nm using UV-visible spectrophotometer.

Fig. 3. UV-visible spectra of curcumin extracted from turmeric powder and curcumin (HIMEDIA Co.).

The UV- visible spectra of curcumin represent the transition between the electronic energy levels. The maximum absorption wavelength of a compound is a measure of the difference between energy levels of the orbitals concerned. An isolated double bond/lone pair produces strong absorption maximum around 190 nm, whereas the presence of conjugation decreases the energy separation between orbitals and give rise to the absorption at longer wavelengths. In organic solvents enolization of diketone of curcumin conjugates between the π-electron clouds of the two vinylguaiacol parts leading to a common conjugated chromophore, resulted in decrease in energy. As a result of low-energy π- π* excitation of that chromophore, curcumin in organic solvents (primarily in methanol or ethanol) typically absorbs around ~420 nm and appears in yellow color [31].

The FTIR spectra of curcumin (HIMEDIA Co.) and curcumin derived from turmeric powder are shown in Fig. 4. The differences in the 3100-3600 cm^{-1} range may be attributed to the OH stretching of the methanol molecules adsorbed in the curcumin derived from turmeric powder [32]. The appearance of strong peak at 1582 cm^{-1} and no peak at 1317 cm^{-1} in the derived curcumin as well as various displacements of the peaks may be due to different interactions between functional groups of curcumin. As shown in Fig. 5, the chemical composition of the

extracted curcumin is a mixture of curcuminoids (curcumin, demethoxycurcumin and bis-demethoxycurcumin).

Fig. 4. FTIR spectra of curcumin (HIMEDIA Co.) and curcumin derived from turmeric.

Fig. 5. Curcuminoids present in turmeric powder.

The IR spectrum of curcumin derived from turmeric is more similar to the IR spectrum of crystalline curcumin derived from turmeric powder (extracted using actone/ethanol/methanol), which was reported in previous studies [32, 33]. A broad peak at 3380 cm^{-1} indicates the presence of –OH group. In the highest frequency region, phenolic vibrations of the curcumin has theoretical frequency at 3595 cm^{-1}, but in practice this band could be shifted downwards due to the intramolecular and intermolecular hydrogen bonds [33, 34]. The appearance of bands with low intensity in the region from 2700-3000 cm^{-1} can be attributed to the C-H stretches [33]. The highest frequency bands observed within 2700-3000 cm^{-1} region are assigned to the aromatic C H stretches, while the lower frequency bands are attributed to the methyl group motions [34]. The peak at 1679 cm^{-1} appeared due to the C=O vibrations [33]. The band at 1623 cm^{-1} can be assigned to the ν(C=C) of the benzene ring [35]. The strong peak at 1582 cm^{-1} has a predominantly mixed ν(C=C) and ν(C=O) characteristic. The most prominent band in the IR spectrum is at 1509 cm^{-1}. This can be attributed to highly mixed vibrations ($^{\nu}$C=O, $^{\delta}$CC^{10}C, $^{\delta}$CC=O) [33]. The peaks at 1430 cm^{-1} appeared due to the asymmetric angular deformation vibrations of methyl groups [34]. The observed bands at 1377 cm^{-1} and 1207 cm^{-1} can be attributed to ν(C-O) and δ(C=C-H) of interring chain, respectively. One band and one shoulder at 1270/1238 cm^{-1} and peak at 1167 cm^{-1} are attributed to the in-plane deformation vibrations of (CCH) of phenyl rings and skeletal in-plane deformations, respectively. A prominent band at

1124 cm^{-1} is assigned also to the (C-O-C) vibrations [33]. The peak at 1031 cm^{-1} appeared due to C-O stretching coupling with the adjacent C-C stretching vibrations [32]. The bands at 964 cm^{-1} and 815 cm^{-1} assigned to the ν(C-O) vibrations. The IR bands at 815 cm^{-1} and 720 cm^{-1} belongs to the ν(C-H) out of plane vibration of the aromatic ring [34]. In the range of 700-500 cm^{-1}, we could see deformation vibrations of both benzene rings and the out of plane vibrations of both OH groups, which are at 607 cm^{-1} and 546 cm^{-1} [33].

3.2. Characterization of curcumin entrapped chitosan/nanocellulose/Tween 20 hydrogels

3.2.1. FTIR analysis

Fig. 6 displays the FTIR spectra of curcumin (extracted), Tween 20, and curcumin/Tween 20 incorporated chitosan based hydrogel. From the spectrum of curcumin/Tween 20 incorporated chitosan hydrogel, it can be seen that the bands corresponded to the functional groups of Tween 20 are more prominent together with the bands assigned to the functional groups of the hydrogel. The sharper peaks related to the functional groups of curcumin are super imposed by the broader peaks of Tween 20 and chitosan hydrogel [35] (in the spectrum of curcumin/Tween 20 incorporated hydrogel). Also, the drug concentration loaded to the hydrogel is very low when compared to Tween 20 concentration. Therefore, the peaks related to Tween 20 are more prominent in the spectrum of curcumin/Tween 20 incorporated hydrogel. However, there are no new peaks appeared in the spectrum of curcumin/Tween 20 incorporated hydrogel.

Fig. 6. FTIR spectra of curcumin (extracted), Tween 20, nanocellulose reinforced chitosan hydrogel and curcumin/Tween 20 incorporated hydrogel.

3.2.2. Morphology studies

The morphology of 0.5% CNC-chitosan hydrogels formed at atmospheric condition and high-pressure conditions (50 bar) was examined using field emission scanning electron microscope. The micrographs of the cross section of hydrogels are shown in Fig.7. The micrographs clearly show the porous network of the gels. As shown in Fig. 7a, hydrogel formed at atmospheric condition showed closed pore structures with around 100-300 μm pore size. After the gas foaming, the pore size of the hydrogel significantly increased (more than 10-fold higher compared to the hydrogel formed at atmospheric condition) with the formation of interconnected pore network structures (Fig. 7b).

Fig. 7. Micrographs of a) hydrogel formed at atmospheric condition and b) gas foamed hydrogel

Skin layer formation and poor pore interconnectivity are common issues in porous fabrication techniques. However, these can be overcome by fabrication of polymer matrices using gas foaming method [37]. The porous structure is generated when the discontinuous dispersed gas phase is removed from the continuous phase of polymer. These polymeric foams have low kinetic stability due to the significant difference between the densities of the gas and liquid. The liquid phase tends to move down while the gas tends to move upwards, which leads to the formation of interconnected porous structure with highly porous top surface [38].

3.3 Drug delivery studies

3.3.1. Entrapment efficiency

The drug entrapment efficiency of the hydrogel with different concentrations of surfactant was studied and the results are shown in Fig. 8. To form curcumin loaded hydrogel, 1.5 mg of curcumin was entrapped in 2.50 g of hydrogel (disc diameter 1.8 cm and height 1.2 cm). The hydrogel with 0% (w/v) surfactant revealed the highest drug entrapment efficiency value of 92.09% ± 0.15%, whereas hydrogel containing 30% (w/v) Tween 20 demonstrated the least value of 70.21% ± 0.26%. The percentage entrapment efficiency decreased significantly from 92.09% ± 0.15% to 77.92% ± 0.70% with the addition of 5% (w/v) surfactant to the hydrogel. After that, it slightly decreased from 77.92% ± 0.70% to 70.21% ± 0.26% with increasing the surfactant concentration from 5% to 30% (w/v).

Fig. 8. Entrapment efficiency of curcumin for gas foamed hydrogel and hydrogel formed at atmospheric condition.

Similar results were obtained by Petchsomrit, Sermkaew and Wiwattanapatapee [18] for oil entrapped alginate bead formulation of curcumin. Tween 80 was used as the surfactant for their study and the entrapment efficiency of curcumin was found to decrease from 73.69% ± 2.04% to 40.28% ± 0.23% with increasing the Tween 80 content from 0% to 30%. From the study of variability of (poly lactic-co-glycolic acid) PLGA nanoparticles quality of protein loaded PLGA nanoparticles by Plackett–Burman design, Rahman, Zidan, Habib and Khan [39] described that the decreasing of the entrapment efficiency with increasing the surfactant is due to the fact that the higher concentration of the emulsifier increases the partition of the drug from internal to external phase due to the increased solubility of the drug in the external phase. In addition, the alkyl chain length influences the hydrophile–lipophile balance (HLB) value of the surfactant, which in turn directly affects the drug entrapment efficiency [13]. Non-ionic surfactants have hydrophilic and lipophilic properties and are characterized by its' hydrophile–

lipophile balance values. Low HLB value corresponds to high hydrophobicity. The higher HLB value the more water soluble the surfactant [40]. The lower the HLB of the surfactant the higher will be the drug entrapment efficiency as in the case of niosomes prepared using Span 60 (HLB = 4.7), compared with Span 40 with a higher HLB of 6.7 [41-43]. The HLB value of Tween 20 is 16.7. The higher HLB value represents higher hydrophilic property. According to Dinarvand, Moghadam, Sheikhi and Atyabi [44], the higher internal aqueous volume may increase the volume of water droplets in the hydrophobic phase. This will promote more contact and exchange (drug loss) to the external water phase. Polymer phase acts as a diffusion barrier against movement of drug molecules between the internal and external aqueous phases; the thickness of this layer decreases when the internal aqueous volume is increased. This may lead to the reduction of drug entrapment efficiency.

In this study, we have compared the drug delivery behavior of the gas foamed hydrogel with the hydrogel prepared at atmospheric condition. As can be seen from the Fig. 8, the entrapment efficiency of curcumin in gas foamed hydrogel is slightly lower than that of the hydrogel formed at atmospheric condition. This result is different compared to our previous study [8], which has reported that the gas foamed hydrogel has higher drug entrapment efficiency compared to hydrogel formed in atmospheric condition. This may be caused by the different drug loading methods that have been applied in these two different studies. In previous study [8], the drug was encapsulated by post-loading method. However, in this study we are applying in situ loading method for the comparative study between the hydrogels prepared under gas foamed and atmospheric condition. In situ loading method is used in this study to incorporate both of the surfactant and the drug to the hydrogel matrix. This in situ loading method does not perform the same as the previous post-loading method [44]. From the studies on the effects of

different drug loading methods on drug delivery, Wong and Dodou [45] reported that the drug is embedded within polymeric network when in situ loaded, instead of being deposited in microporous spaces of the hydrogel when post loaded method was applied. As can be seen from Fig. 7, the hydrogel prepared at atmospheric condition composed of small pore structures when compared to the gas foamed hydrogel. The decrease of pore size of the hydrogel simply correlated with the higher hydrogel density, which contributing to more embedded drug in the hydrogel matrix and higher encapsulation efficiency. Therefore, in this study, the hydrogel prepared at atmospheric condition showed higher encapsulation efficiency compared to gas foamed hydrogel. Petchsomrit, Sermkaew and Wiwattanapatapee [6] also reported that the higher hydrogel density contributed to the increase of curcumin content on in situ drug loaded, alginate-based composite sponge.

From the comparison between post loaded formulations from our previous study [8] and in situ loaded formulations used in this study, it is found that the in situ loading method provides better drug entrapment efficiency within hydrogel network for all the hydrogel prepared under gas foamed and atmospheric condition due to the specific interactions between polymer and drug molecules [45].

3.3.2. Drug release

3.3.2.1. Drug release from the hydrogel formed at atmospheric condition

The oral bioavailability of a drug relies upon on its solubility and/or dissolution rate, and dissolution can be the rate determining step for the onset of drug action. Hence there are numerous approaches available and reported in literature to enhance dissolution and drug bioavailability of poorly water-soluble drugs [7-10, 46-47]. The use of surfactant to improve the

solubility of hydrophobic/lipophilic drugs is a common practice in the industry and it has been extensively studied by many researchers [46-47]. In this study, curcumin and Tween 20 were incorporated into hydrogel matrix via in-situ loading method to allow hydrogel network formulation and drug encapsulation are accomplished simultaneously.

Fig. 9. Curcumin release from the hydrogels containing different concentrations of Tween 20.

The hydrogel discs (1.2 cm height and 1.8 cm diameter) containing 1.5 mg of drug with different concentrations of Tween 20 (5%, 10%, 15%, 20%, 25% and 30% (w/v)) were immersed in simulated gastric fluid and drug release was monitored over a period of 7.5 h. Since the solubility of curcumin is very low [46], a large volume of the releasing medium was used to maintain a good sink condition [47]. As can be seen in Fig. 9, the cumulative release of curcumin increased from 0.21% ± 0.02% to 54.85% ± 0.77% with increasing the Tween 20 concentration from 0% to 30% (w/v), after 7.5 h immersion. Release studies in the presence of Tween 20 show a burst release profile for curcumin, up to 20% of curcumin released in the first 60 min of the experiment. As shown in Fig. 9, with the increase of Tween 20 concentration from 5-30% (w/v), at a fixed drug concentration, the amount of drug release increased from 31.82% ± 0.75% to 54.85% ± 0.77%. This is almost 1.7-fold increase after 7.5 h. During the time of monitoring, the formulations containing lower amount of Tween 20 produced an incomplete solubilization of curcumin, whereas complete solubilization showed at high concentration of Tween 20. Therefore, larger amount of surfactant produced a higher drug release. Ratanajiajaroen and Ohshima [7] showed that the solubility of curcumin increased from 11 mg/mL to 0.767 mg/mL with Tween 20, at a concentration of 2% (v/v) in acetate buffer (pH 5.5). In addition, they found that the drug release rate increased from chitin beads as the Tween 20 concentration increased. O'Toole, Henderson, Soucy, Fasciotto, Hoblitzell, Keynton, Ehringer and Gobin [17]

investigated that the curcumin saturation point increased linearly with Tween 20 concentration throughout the range used in their experiments with an upper limit of 294 μM curcumin with 0.05% (w/v) Tween 20. Further, they reported that curcumin can be released completely from the submicrometer spray-dried chitosan/Tween 20 particles in both 1% acetic acid and phosphate buffered saline solutions over a 2 h period.

Moreover, in terms of therapeutic applications for abdominal disorders, the doses of curcumin up to the healing levels should also been concerned. Considering the strong association of *H. pylori* and gastric cancer the authors of the study by Mahady, Pendland, Yun and Lu [4] showed that both curcumin and methanolic extract of turmeric rhizome inhibited the growth of 19 different strains of *H. pylori.* They reported that curcumin inhibited the growth of all the *H.pylori* strains by 100% at a concentration of 12.5 μg/mL with a minimum inhibitory concentration from 6.25-12.5 μg/mL. De, Kundu, Swarnakar, Ramamurthy, Chowdhury, Nair and Mukhopadhyay [3] investigated that the minimum inhibitory concentration of curcumin for *H.pylori* strains ranged from 5 μg/mL to 50 μg/mL, and the majority of the strains (81%) showed a minimum inhibitory concentration of either 10 μg/mL (23%) or 15 μg/mL (58%). In addition, curcumin is able to suppress the proliferation and survival of cancer cells by directly or indirectly binding to various cellular molecular targets [48]. Liu, Xiang, Wu and Wang [49] reported that curcumin inhibited the growth of gastric cancer cells in a concentration and a time-dependent manner. Their studies showed that as compared to untreated cancer cells, the cell proliferation was significantly inhibited in the curcumin treated samples after 48 h of treatment with 50 μM curcumin. In our study, the maximum concentration of curcumin released in the simulated gastric fluid was 3.98 μg/mL after 7.5 h. Even so, we found that the drug release of the hydrogel increased (≥10 μg/mL) with increasing the initial concentration of the drug which incorporated to the hydrogel

(for same Tween 20 concentration). However, with increasing the initial amount of drug, the percentage release of drug dramatically decreased during the period of monitoring. Therefore, 1.5 mg of drug per hydrogel disc (1.2 cm height and 1.8 cm diameter) was used for the encapsulation in this study. However, the initial drug loading amount to the hydrogel can be varied in order to get the drug release to the extent desired (to reach the therapeutic levels) or to obtain the minimum inhibitory concentration. As a summary from the results obtained from drug release studies, the nanocellulose reinforced chitosan/Tween 20 hydrogel can be suggested as a promising candidate for carrying curcumin for the absorption of stomach and upper intestinal tract.

3.3.2.2. Drug release from gas foamed hydrogel

Fig. 7b has clearly illustrates that nanocellulose reinforced chitosan hydrogel fabricated using carbon dioxide gas foaming process possess large-scale macroporous with wide interconnected pores and large accessible surface area. Due to the large pore size of hydrogels, a rapid initial burst release of drug was typically observed as observed in previous study [8].

Fig. 10. Curcumin release from gas foamed hydrogel and hydrogels formed at atmospheric condition with different concentrations of Tween 20.

As shown in Fig. 10, the concentration of released drug from gas foamed hydrogel was greater when compared to the hydrogel formed at atmospheric condition within the first 120 minutes. The increased pore size and pore interconnectivity of gas foamed hydrogel act as a capillary system causing a rapid diffusion of drug solution through the hydrogel matrix [50]. At 60 minutes, For the hydrogel containing 5% (w/v) Tween 20, the cumulative release of drug at 60 minutes was 8.51% ± 0.61% and 7.95% ± 0.39% for gas foamed hydrogel and hydrogel

formed at atmospheric condition respectively. While, the cumulative release of drug at 60 minutes was 21.58% ± 0.32% and 20.87% ± 0.46% respectively for hydrogel containing 30% (w/v) Tween 20 prepared under gas foam and at atmospheric condition. After the burst release, the rate of drug release of both types of hydrogels become almost similar.

From our previous study [8], the gas foamed hydrogel showed higher drug release when compared to the hydrogel formed at atmospheric condition. However, gas foamed hydrogel did not show any improvement of the drug release over the hydrogel formed at atmospheric condition in this study. Kawase, Michibayashi, Nakashima, Kurikawa, Yagi and Mizoguchi [51] reported that the permeation rates of the drug from post-loaded formulations are generally more rapid compared to the in situ loaded ones. This may be due to drug being deposited in microporous spaces of the hydrogel when post-loaded instead of being embedded within polymeric network when loaded in situ. In our previous study by applying post-loading method, gas foamed hydrogel with large and interconnected pore structures has allowed the drug deposited in the pore spaces of the hydrogel to be easily transported [52]. Therefore, the prepared gas foamed hydrogel with post-loading method has attributed to higher drug release compared to the hydrogel prepared at atmospheric condition in the previous study [8].

In the current research work, we have applied in situ loading method for the drug loading. The gas foamed hydrogel with larger interconnected pore structures would cause less impact on the drug release from the in situ loaded formulations [44, 45, 52]. Therefore, the gas foamed hydrogel did not show any improvement of the drug release over the hydrogel formed at atmospheric condition in this study.

3.4. Drug activity

The chemical reactivity and biological activity of the drug are the most critical parameters in drug delivery systems after drug release process [30]. Curcumin has three reactive functional groups which associated with its different biological activities: one diketone moiety, and two phenolic groups. The presence of C=O groups as hydrogen acceptors and C-4 as a hydrogen donor are the important chemical reactions associated with its biological activities [53-54].

Fig. 11. UV-visible spectra of (a) pure drug and (b) released drug.

As shown in Fig. 11a and 11b, both of the UV-visible spectra indicate absorption peak around 427 nm. This can be assigned to the low-energy π- π* excitation of the chromophore which formed due to the enolization of the diketone group and conjugation between the π-electron clouds of the two vinylguaiacol [31]. The presence of the absorption peak around 427 nm in both of the spectra revealed that the reactive functional groups which associated with the biological activity of curcumin retained without any deterioration due to any denaturation reaction with the carrier molecules.

3.5. Solubility study

From our previous study [8,10], we observed lower drug release profiles of the hydrogel due to poor solubility of curcumin in simulated gastric fluid. To improve curcumin's solubility, Tween 20 was selected as potential solubilizing agent due to its biocompatibility and previous successful application in curcumin drug delivery systems [16, 17, 55].

Fig. 12. Solubility of curcumin in simulated gastric fluid with different concentrations of Tween 20.

The ability of Tween 20 to solubilize curcumin in simulated gastric fluid was evaluated by measuring the curcumin concentration in curcumin-saturated simulated gastric fluid with various amounts of Tween 20. As shown in Fig. 12, the solubility of the drug gradually increased with increasing the concentration of nonionic surfactant (Tween 20), with an upper limit of 3.014 ± 0.041 mg/mL in the presence of 3.2% (w/v) Tween 20. Similar results were obtained from the studies on solubility of curcumin in aqueous polysorbate micelle reported by Inchai, Ezure, Hongwiset and Yotsawimonwat [56]. Their studies had showed that the solubility of curcumin increased up to 2.7 mg/mL in 20% aqueous solution of Tween 20. O'Toole, Henderson, Soucy, Fasciotto, Hoblitzell, Keynton, Ehringer and Gobin [17] showed that the saturation point of curcumin increased linearly with increasing the Tween 20 concentration in 1% acetic acid medium. Their findings revealed that the solubility of curcumin increased to an upper limit of 294 μM (~0.108 mg/L) with 0.05% (w/v) Tween 20.

With higher pH, curcumin degrades rapidly (on the timescale of minutes). However, the solubility of curcumin decreases rapidly with decreasing of pH [56-57]. In our study, the solubility of curcumin in simulated gastric medium was ~6 μg/mL (without addition of the surfactant). It showed a slight decrease when compared to the results obtained by Hung, Chen, Lee, Sun, Lee and Huang [58] which was 25 μM (~9.2 μg/mL) in pH 7 buffer solution. This may be due to the low pH of the simulated gastric fluid.

4. Conclusions

In this study, curcumin was extracted from dried rhizomes of *curcuma longa* using methanol for preparation of curcumin loaded chitosan/nanocellulose/Tween20 hydrogel. As a result of low-energy π- π* excitation of the chromophore, both curcumin (HIMEDIA Co.) and curcumin

(extracted) showed typical absorption peaks around 420 nm in the UV-visible spectrum. The drug release of the hydrogel increased from 0.21% ± 0.02% to 54.85% ± 0.77% with increasing of Tween 20 concentration from 0% to 30% (w/v) after 7.5 h immersion. FESEM micrographs had proven that the pore size of the hydrogel increased more than tenfold after the gas foaming process (at 50 bar). Gas foamed hydrogel showed a high burst release of the drug compared to the hydrogel formed at atmospheric condition. The entrapment efficiency of the hydrogels decreased with increasing the Tween 20 concentration. Solubility studies showed that the saturation point of curcumin increased linearly with increasing the concentration of nonionic surfactant (Tween 20). The mavimum limit of 3.014 ± 0.041 mg/mL was achieved with the introduction of 3.2% (w/v) of Tween 20. Furthermore, curcumin retained its structural integrity after release to the gastric medium, which is a critical requirement for preserving drug activity. The solubility of a drug is a fundamental parameter in terms of promoting any effect impacting the therapeutic effect of the drug. Thus, the Tween 20 incorporated chitosan/nanocellulose hydrogel has provided promising platform as a carrier for curcumin with improved solubility characteristics for the absorption from stomach and upper intestinal tract. Since biocompatibility of the hydrogel system is a critical concern for researchers in drug delivery field. Therefore, investigations on the cytotoxicity and biocompatibility of the Tween 20 incorporated chitosan/nanocellulose hydrogel for in vivo drug delivery applications will be conducted in future works.

Acknowledgments: The authors would like to acknowledge the financial support from the Ministry of Education Malaysia: FP053-2015A and PR005-2017A; and University Malaya research grant: PG160-2016A, RU005D-2016, and ST012-2017 and RU018I-2016 and International Funding AUA Scholars IF025-2018 for the success of this project.

References

[1] D. Madhavi, D. Kagan, Bioavailability of a sustained release formulation of curcumin, Integrative Medicine: A Clinician's Journal 13(3) (2014) 24.

[2] S. Zorofchian Moghadamtousi, H. Abdul Kadir, P. Hassandarvish, H. Tajik, S. Abubakar, K. Zandi, A review on antibacterial, antiviral, and antifungal activity of curcumin, BioMed research international 2014 (2014).

[3] R. De, P. Kundu, S. Swarnakar, T. Ramamurthy, A. Chowdhury, G.B. Nair, A.K. Mukhopadhyay, Antimicrobial activity of curcumin against Helicobacter pylori isolates from India and during infections in mice, Antimicrobial agents and chemotherapy 53(4) (2009) 1592-1597.

[4] G. Mahady, S. Pendland, G. Yun, Z. Lu, Turmeric (Curcuma longa) and curcumin inhibit the growth of Helicobacter pylori, a group 1 carcinogen, Anticancer research 22(6C) (2002) 4179-4181.

[5] N.A. Mohammed, N.Y. Habil, Evaluation of antimicrobial activity of curcumin against two oral bacteria, Automation, Control and Intelligent Systems 3(2-1) (2015) 18-21.

[6] A. Petchsomrit, N. Sermkaew, R. Wiwattanapatapee, Alginate-based composite sponges as gastroretentive carriers for curcumin-loaded self-microemulsifying drug delivery systems, Scientia pharmaceutica 85(1) (2017) 11.

[7] P. Ratanajiajaroen, M. Ohshima, Synthesis, release ability and bioactivity evaluation of chitin beads incorporated with curcumin for drug delivery applications, Journal of microencapsulation 29(6) (2012) 549-558.

[8] T.M.S. Udeni Gunathilake, Y.C. Ching, C.H. Chuah, Enhancement of curcumin bioavailability using nanocellulose reinforced chitosan hydrogel, Polymers 9(2) (2017) 64.

[9] Y.C. Ching, A. Ershad, C.A. Luqman, K.W. Choo, C.K. Yong, J.J. Sabariah, C.H. Chuah, N.S. Liou, Rheological properties of cellulose nanocrystal-embedded polymer composites: A review. Cellulose 23 (2016**)** 1011–1030.

[10] U.T.M. Sampath, Y.C. Ching, C.H. Chuah, R. Singh, P.-C. Lin, Preparation and characterization of nanocellulose reinforced semi-interpenetrating polymer network of chitosan hydrogel, Cellulose 24(5) (2017) 2215-2228.
[11] K.W.Choo, Y.C. Ching, C.H. Chuah, J. Sabariah, N.S. Liou, Preparation and characterization of polyvinyl alcohol-chitosan composite films reinforced with cellulose nanofiber, Materials 9 (8 (2016) 644.
[12] J. Lu, X. Li, R. Yang, J. Zhao, Y. Qu, Tween 40 pretreatment of unwashed water-insoluble solids of reed straw and corn stover pretreated with liquid hot water to obtain high concentrations of bioethanol, Biotechnology for biofuels 6(1) (2013) 159.
[13] M.S. El-Ridy, A. Abdelbary, T. Essam, R.M. Abd EL-Salam, A.A. Aly Kassem, Niosomes as a potential drug delivery system for increasing the efficacy and safety of nystatin, Drug development and industrial pharmacy 37(12) (2011) 1491-1508.
[14] A. Abdelbary, T. Essam, R. Abd El-Salam, A. AlyKassem, Niosomes as a potential drug delivery system for increasing the efficacy and safety of nystatin (antifungal), Drug Dev Ind Pharm 37 (2011) 149-508.
[15] S. Mehta, G. Kaur, K. Bhasin, Tween-embedded microemulsions—physicochemical and spectroscopic analysis for antitubercular drugs, AAPS PharmSciTech 11(1) (2010) 143-153.
[16] P. Ratanajiajaroen, A. Watthanaphanit, H. Tamura, S. Tokura, R. Rujiravanit, Release characteristic and stability of curcumin incorporated in β-chitin non-woven fibrous sheet using Tween 20 as an emulsifier, European Polymer Journal 48(3) (2012) 512-523.
[17] M.G. O'Toole, R.M. Henderson, P.A. Soucy, B.H. Fasciotto, P.J. Hoblitzell, R.S. Keynton, W.D. Ehringer, A.S. Gobin, Curcumin encapsulation in submicrometer spray-dried chitosan/Tween 20 particles, Biomacromolecules 13(8) (2012) 2309-2314.
[18] A. Petchsomrit, N. Sermkaew, R. Wiwattanapatapee, Effect of alginate and surfactant on physical properties of oil entrapped alginate bead formulation of curcumin, International Journal of Medical, Health, Biomedical, Bioengineering and Pharmaceutical Engineering 7(12) (2013) 864-868.
[19] T. Cserháti, E. Forgács, G. Oros, Biological activity and environmental impact of anionic surfactants, Environment international 28(5) (2002) 337-348.
[20] A.A.H. Sathali, G. Rajalakshmi, Evaluation of transdermal targeted niosomal drug delivery of terbinafine hydrochloride, Int J Pharm Tech Res 2(3) (2010) 2081-2089.
[21] K. Prabhakar, S.M. Afzal, G. Surender, V. Kishan, Tween 80 containing lipid nanoemulsions for delivery of indinavir to brain, Acta Pharmaceutica Sinica B 3(5) (2013) 345-353.
[22] A. Petchsomrit, N. Sermkaew, R. Wiwattanapatapee, Effect of alginate and surfactant on physical properties of oil entrapped alginate bead formulation of curcumin, World Academy of Science, Engineering and Technology, International Journal of Medical, Health, Biomedical, Bioengineering and Pharmaceutical Engineering 7(12) (2013) 864-868.
[23] T. Ren, N. Xu, C. Cao, W. Yuan, X. Yu, J. Chen, J. Ren, Preparation and therapeutic efficacy of polysorbate-80-coated amphotericin B/PLA-b-PEG nanoparticles, Journal of Biomaterials Science, Polymer Edition 20(10) (2009) 1369-1380.
[24] Y. Shahzad, S. Saeed, M.U. Ghori, T. Mahmood, A.M. Yousaf, M. Jamshaid, R. Sheikh, S.A. Rizvi, Influence of polymer ratio and surfactants on controlled drug release from cellulosic microsponges, International journal of biological macromolecules (2017).
[25] M.S. Baig, A. Ahad, M. Aslam, S.S. Imam, M. Aqil, A. Ali, Application of Box–Behnken design for preparation of levofloxacin-loaded stearic acid solid lipid nanoparticles for ocular

delivery: Optimization, in vitro release, ocular tolerance, and antibacterial activity, International journal of biological macromolecules 85 (2016) 258-270.
[26] C.S.F. Picone, R.L. Cunha, Formation of nano and microstructures by polysorbate–chitosan association, Colloids and Surfaces A: Physicochemical and Engineering Aspects 418 (2013) 29-38.
[27] D. Jansirani, R. Saradha, N. Salomideborani, J. Selvapriyadharshini, Comparative evaluation of various extraction methods of curcuminoids from Curcuma longa, Journal of Chemical and Pharmaceutical Sciences (4) (2014) 286-288.
[28] A.L. Parize, H.K. Stulzer, M.C.M. Laranjeira, I.M.d.C. Brighente, T.C.R.d. Souza, Evaluation of chitosan microparticles containing curcumin and crosslinked with sodium tripolyphosphate produced by spray drying, Química Nova 35(6) (2012) 1127-1132.
[29] S. Li, X. Lin, K. Xu, J. He, H. Yang, H. Li, Co-grinding effect on crystalline zaltoprofen with β-cyclodextrin/cucurbit [7] uril in tablet formulation, Scientific Reports 7 (2017).
[30] S. Bashir, Y.Y. Teo, S. Ramesh, K. Ramesh, Synthesis, characterization, properties of N-succinyl chitosan-g-poly (methacrylic acid) hydrogels and in vitro release of theophylline, Polymer 92 (2016) 36-49.
[31] F. Zsila, Z. Bikádi, M. Simonyi, Circular dichroism spectroscopic studies reveal pH dependent binding of curcumin in the minor groove of natural and synthetic nucleic acids, Organic & biomolecular chemistry 2(20) (2004) 2902-2910.
[32] R. Fugita, D. Gálico, R. Guerra, G. Perpétuo, O. Treu-Filho, M. Galhiane, R. Mendes, G. Bannach, Thermal behaviour of curcumin, Braz J Therm Anal 1 (2012) 19-23.
[33] V.T. Bich, N.T. Thuy, N.T. Binh, N.T.M. Huong, P.N.D. Yen, T.T. Luong, Structural and spectral properties of curcumin and metal-curcumin complex derived from turmeric (Curcuma longa), Physics and engineering of new materials (2009) 271-278.
[34] T.M. Kolev, E.A. Velcheva, B.A. Stamboliyska, M. Spiteller, DFT and experimental studies of the structure and vibrational spectra of curcumin, International Journal of Quantum Chemistry 102(6) (2005) 1069-1079.
[35] P.K. Mohan, G. Sreelakshmi, C. Muraleedharan, R. Joseph, Water soluble complexes of curcumin with cyclodextrins: Characterization by FT-Raman spectroscopy, Vibrational Spectroscopy 62 (2012) 77-84.
[36] V. Rubentheren, T.A Ward, C.Y. Chee, P. Nair, Physical and chemical reinforcement of chitosan film using nanocrystalline cellulose and tannic acid. Cellulose 22 (2015) 2529–2541.
[37] U.G. Sampath, Y.C. Ching, C.H. Chuah, J.J. Sabariah, P.-C. Lin, Fabrication of porous materials from natural/synthetic biopolymers and their composites, Materials 9(12) (2016) 991.
[38] F. Dehghani, N. Annabi, Engineering porous scaffolds using gas-based techniques, Current opinion in biotechnology 22(5) (2011) 661-666.
[39] Z. Rahman, A.S. Zidan, M.J. Habib, M.A. Khan, Understanding the quality of protein loaded PLGA nanoparticles variability by Plackett–Burman design, International journal of pharmaceutics 389(1) (2010) 186-194.
[40] D. Ag Seleci, M. Seleci, J.-G. Walter, F. Stahl, T. Scheper, Niosomes as nanoparticular drug carriers: fundamentals and recent applications, Journal of Nanomaterials 2016 (2016).
[41] M. Nasr, S. Mansour, N.D. Mortada, A. Elshamy, Vesicular aceclofenac systems: a comparative study between liposomes and niosomes, Journal of Microencapsulation 25(7) (2008) 499-512.

[42] P.A. Bhat, A.A. Dar, G.M. Rather, Solubilization capabilities of some cationic, anionic, and nonionic surfactants toward the poorly water-soluble antibiotic drug erythromycin, Journal of Chemical & Engineering Data 53(6) (2008) 1271-1277.
[43] Z.S. Bayindir, N. Yuksel, Characterization of niosomes prepared with various nonionic surfactants for paclitaxel oral delivery, Journal of pharmaceutical sciences 99(4) (2010) 2049-2060.
[44] R. Dinarvand, S. Moghadam, A. Sheikhi, F. Atyabi, Effect of surfactant HLB and different formulation variables on the properties of poly-D, L-lactide microspheres of naltrexone prepared by double emulsion technique, Journal of microencapsulation 22(2) (2005) 139-151.
[45] R.S.H. Wong, K. Dodou, Effect of drug loading method and drug physicochemical properties on the material and drug release properties of poly (ethylene oxide) hydrogels for transdermal delivery, Polymers 9(7) (2017) 286.
[46] H.H. Tønnesen, J. Karlsen, Studies on curcumin and curcuminoids, Zeitschrift für Lebensmittel-Untersuchung und Forschung 180(5) (1985) 402-404.
[47] Y.W. Cho, J. Lee, S.C. Lee, K.M. Huh, K. Park, Hydrotropic agents for study of in vitro paclitaxel release from polymeric micelles, Journal of Controlled Release 97(2) (2004) 249-257.
[48] S. Zang, T. Liu, J. Shi, L. Qiao, Curcumin: a promising agent targeting cancer stem cells, Anti-Cancer Agents in Medicinal Chemistry (Formerly Current Medicinal Chemistry-Anti-Cancer Agents) 14(6) (2014) 787-792.
[49] G. Liu, T. Xiang, Q.F. Wu, W.X. Wang, Curcumin suppresses the proliferation of gastric cancer cells by downregulating H19, Oncology letters 12(6) (2016) 5156-5162.
[50] T. M. S. Udenni Gunathilake, Y. C. Ching, K. Y. Ching, C. H. Chuah and L. Chuah Abdullah, Biomedical and microbiological applications of bio-Based porous materials: A review, Polymers 9 (160) (2017) 1-16.
[51] M. Kawase, N. Michibayashi, Y. Nakashima, N. Kurikawa, K. Yagi, T. Mizoguchi, Application of glutaraldehyde-crosslinked chitosan as a scaffold for hepatocyte attachment, Biological and Pharmaceutical Bulletin 20(6) (1997) 708-710.
[52] A. Ullah, C.M. Kim, G.M. Kim, Porous polymer coatings on metal microneedles for enhanced drug delivery, Royal Society open science 5(4) (2018) 171609.
[53] M. Ahmed, M.A. Qadir, M.I. Shafiq, M. Muddassar, A. Hameed, M.N. Arshad, A.M. Asiri, Curcumin: Synthesis optimization and in silico interaction with cyclin dependent kinase, Acta Pharmaceutica 67(3) (2017) 385-395.
[54] S. Wang, X. Liu, I.J. Villar-Garcia, R. Chen, Amino acid based hydrogels with dual responsiveness for oral drug delivery, Macromolecular bioscience 16(9) (2016) 1258-1264.
[55] A. Rahma, M.M. Munir, A. Prasetyo, V. Suendo, H. Rachmawati, Intermolecular interactions and the release pattern of electrospun curcumin-polyvinyl (pyrrolidone) fiber, Biological and Pharmaceutical Bulletin 39(2) (2016) 163-173.
[56] N. Inchai, Y. Ezure, D. Hongwiset, S. Yotsawimonwat, Investigation on solubility and stability of curcumin in aqueous polysorbate micelle, International Journal of Management and Applied Science (IJMAS) 3(4) (2015) 157-161.
[57] K. Fimantari, E. Budianto, Effect of drug loading method against drug dissolution mechanism of encapsulated amoxicillin trihydrate in matrix of semi-IPN chitosan-poly (N-vinylpyrrolidone) hydrogel with KHCO3 as pore forming agent in floating drug delivery system, AIP Conference Proceedings, AIP Publishing, 2018, p. 020001.
[58] W.-C. Hung, F.-Y. Chen, C.-C. Lee, Y. Sun, M.-T. Lee, H.W. Huang, Membrane-thinning effect of curcumin, Biophysical journal 94(11) (2008) 4331-4338.

711

712

713

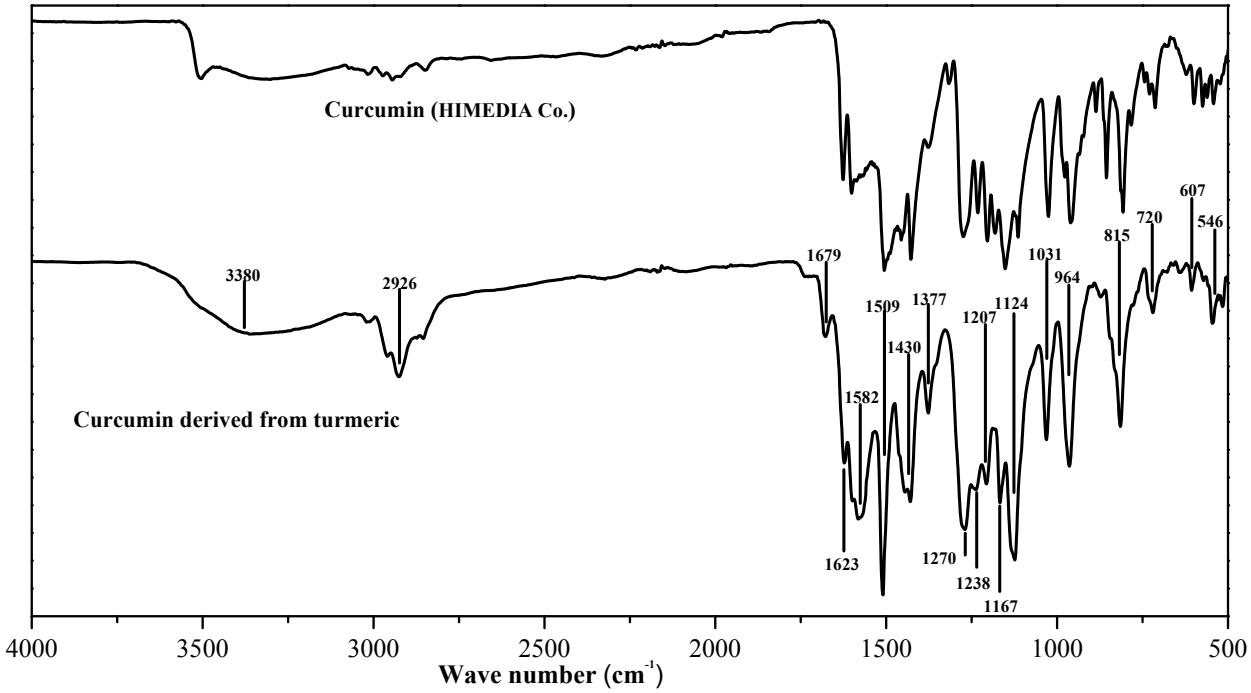

Fig. 1. FTIR spectra of curcumin (HIMEDIA Co.) and curcumin derived from turmeric.

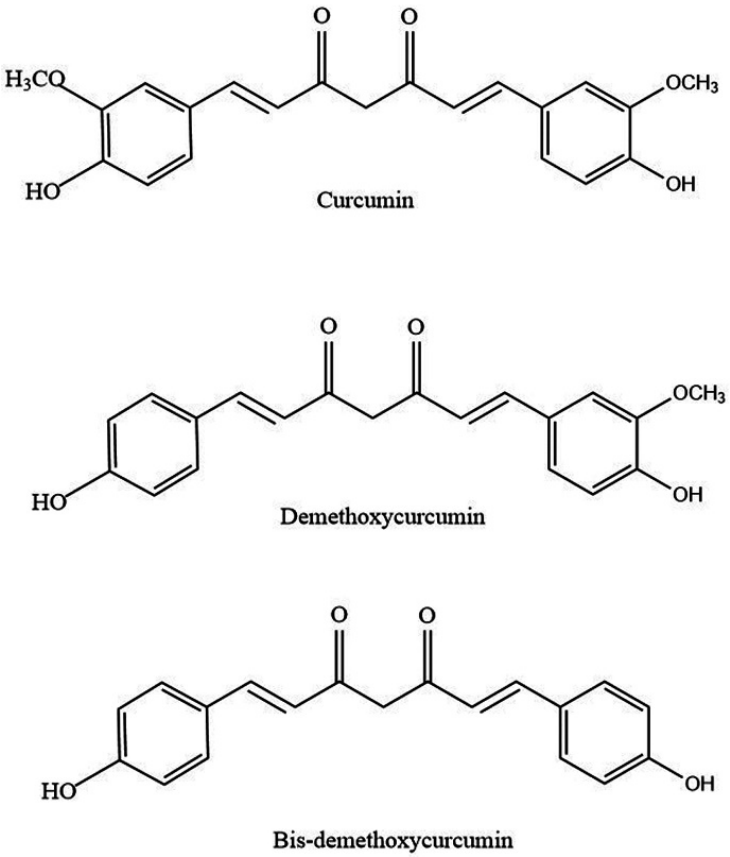

Fig. 2. Curcuminoids present in turmeric powder.

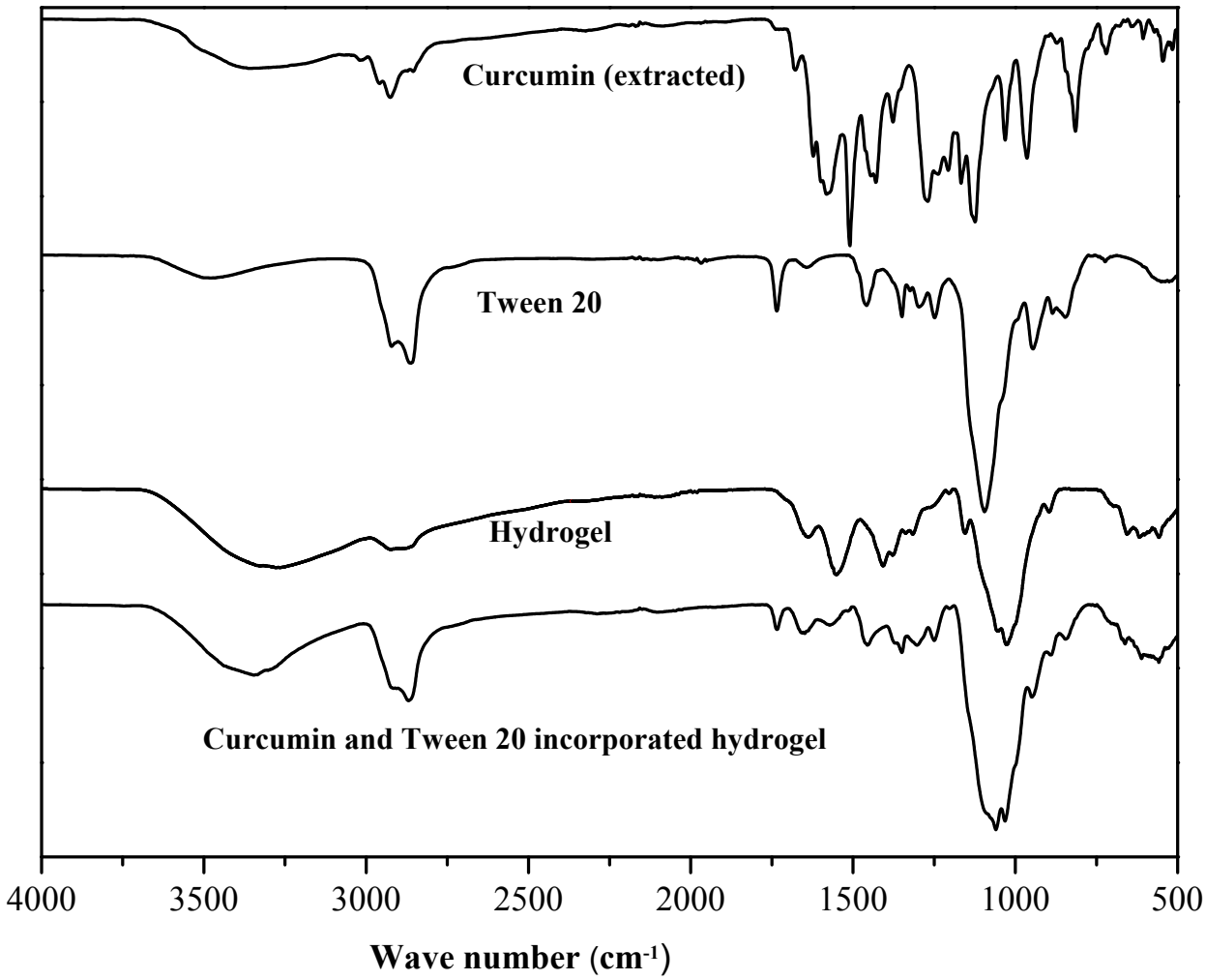

Fig. 3. FTIR spectra of curcumin (extracted), Tween 20, nanocellulose reinforced chitosan hydrogel and curcumin/Tween 20 incorporated hydrogel.

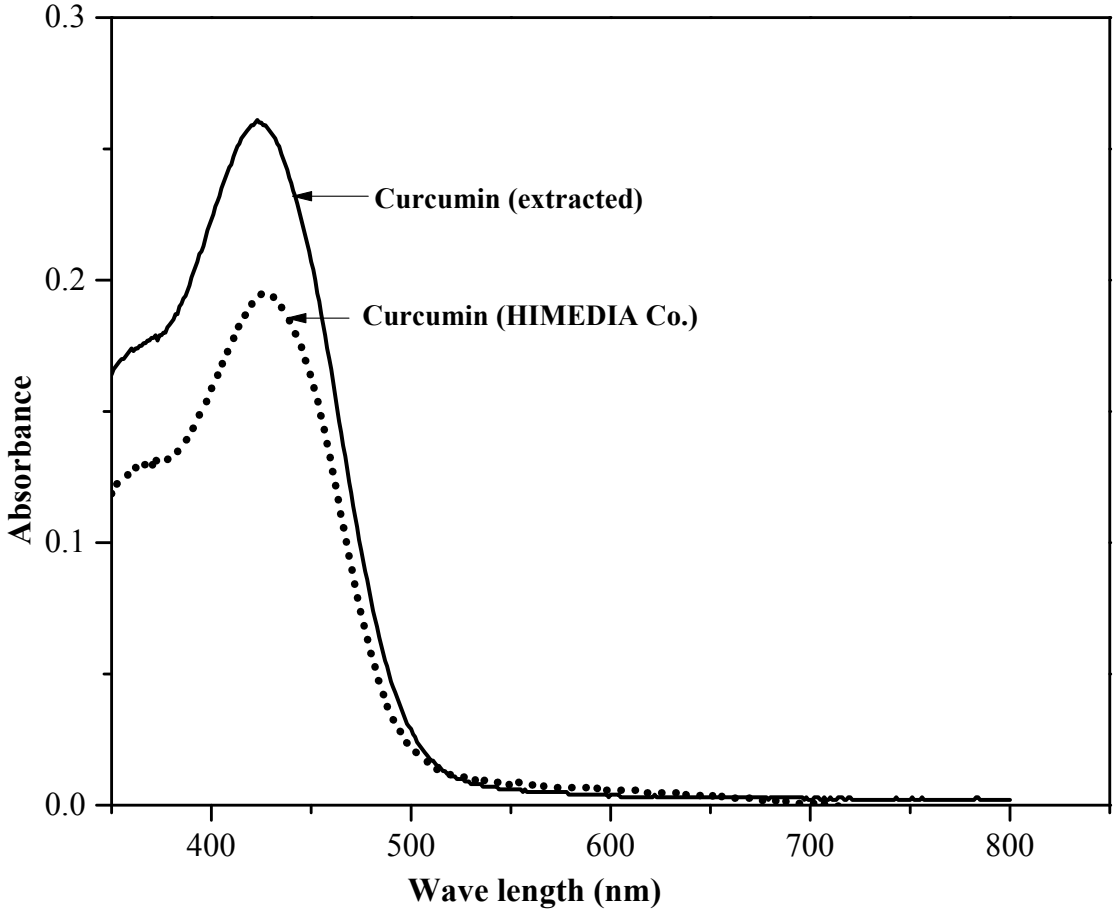

Fig. 4. UV-visible spectra of curcumin extracted from turmeric powder and curcumin (HIMEDIA Co.).

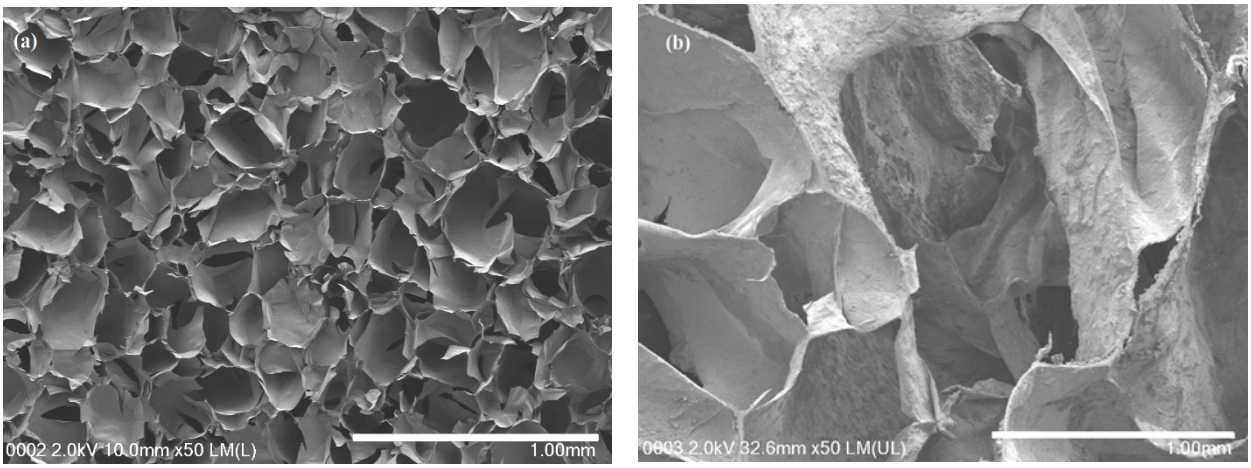

Fig. 5. Micrographs of a) hydrogel formed at atmospheric condition and b) gas foamed hydrogel.

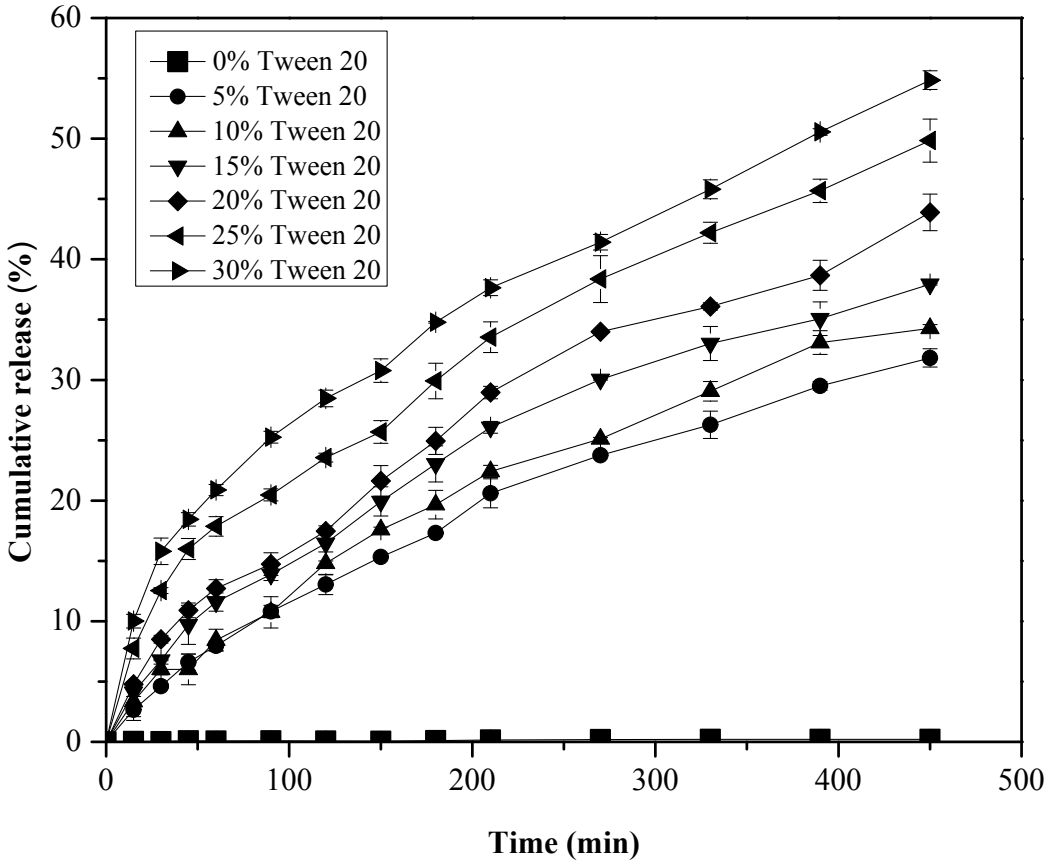

Fig. 6. Curcumin release from the hydrogels containing different concentrations of Tween 20.

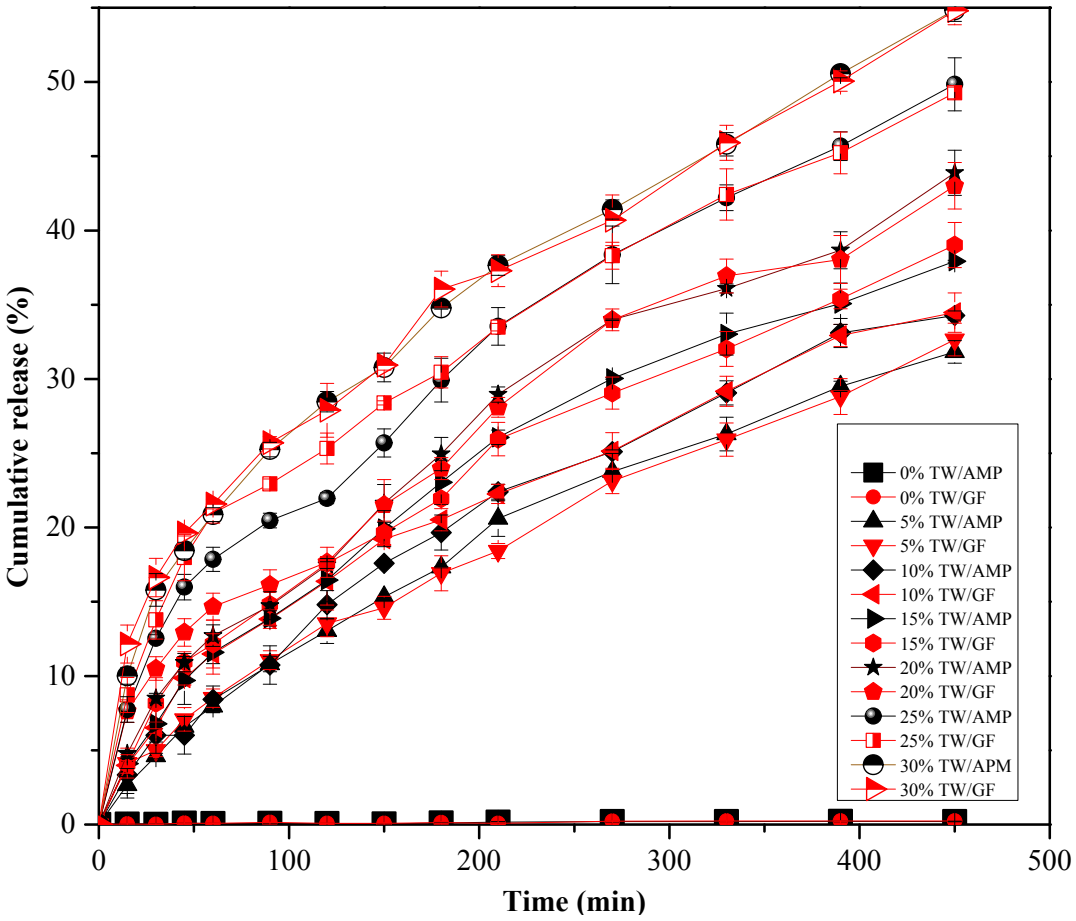

Fig. 7. Curcumin release from the hydrogels formed at atmospheric condition (AMP) and high-pressure condition (GF) with different concentrations of Tween 20 (TW).

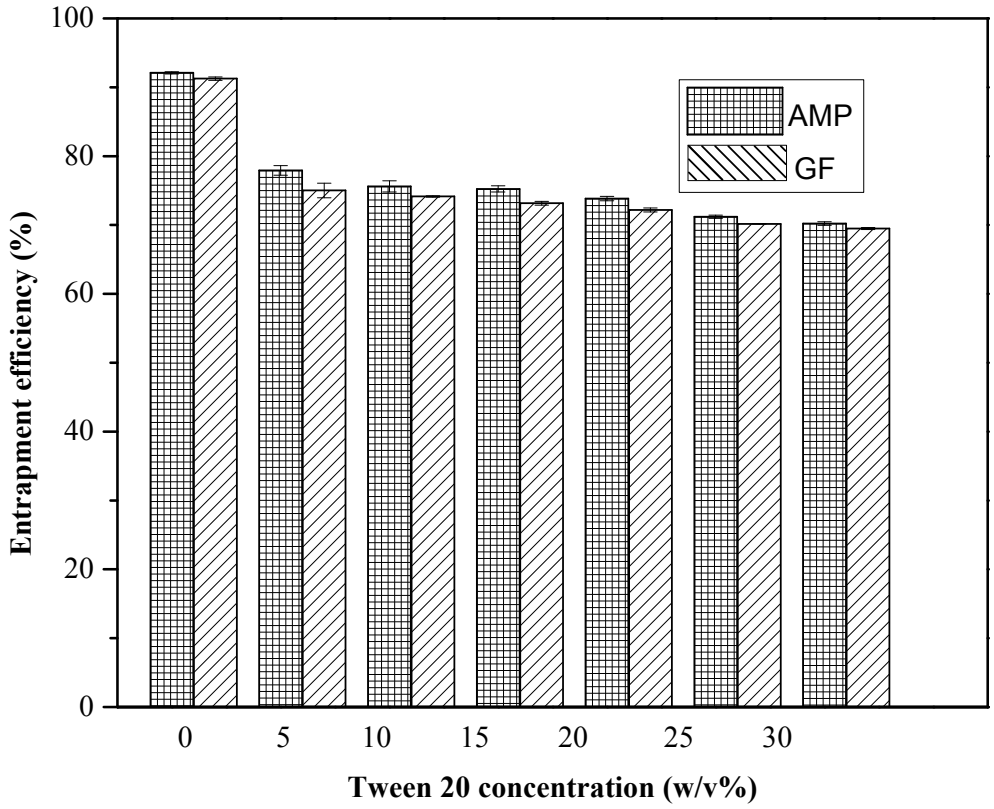

Fig. 8. Entrapment efficiency of curcumin in gas foamed hydrogel (GF) and hydrogel formed at atmospheric condition (AMP).

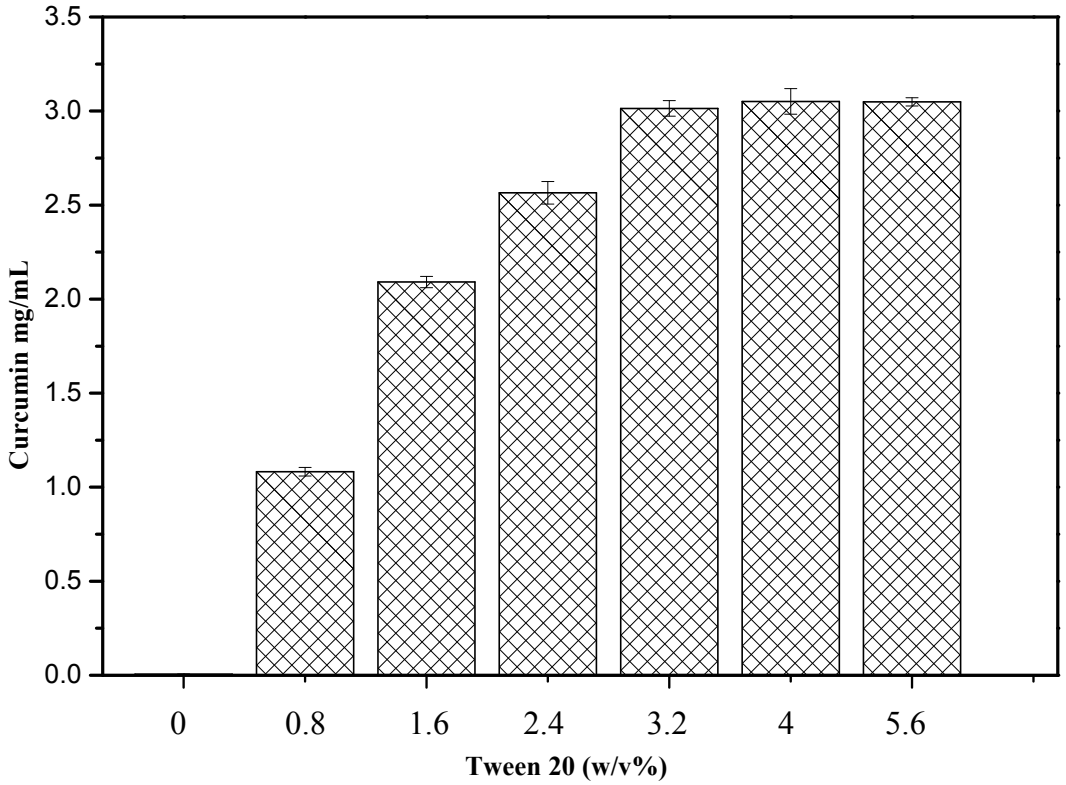

Fig. 9. Solubility of curcumin in simulated gastric fluid with different concentrations of Tween 20.

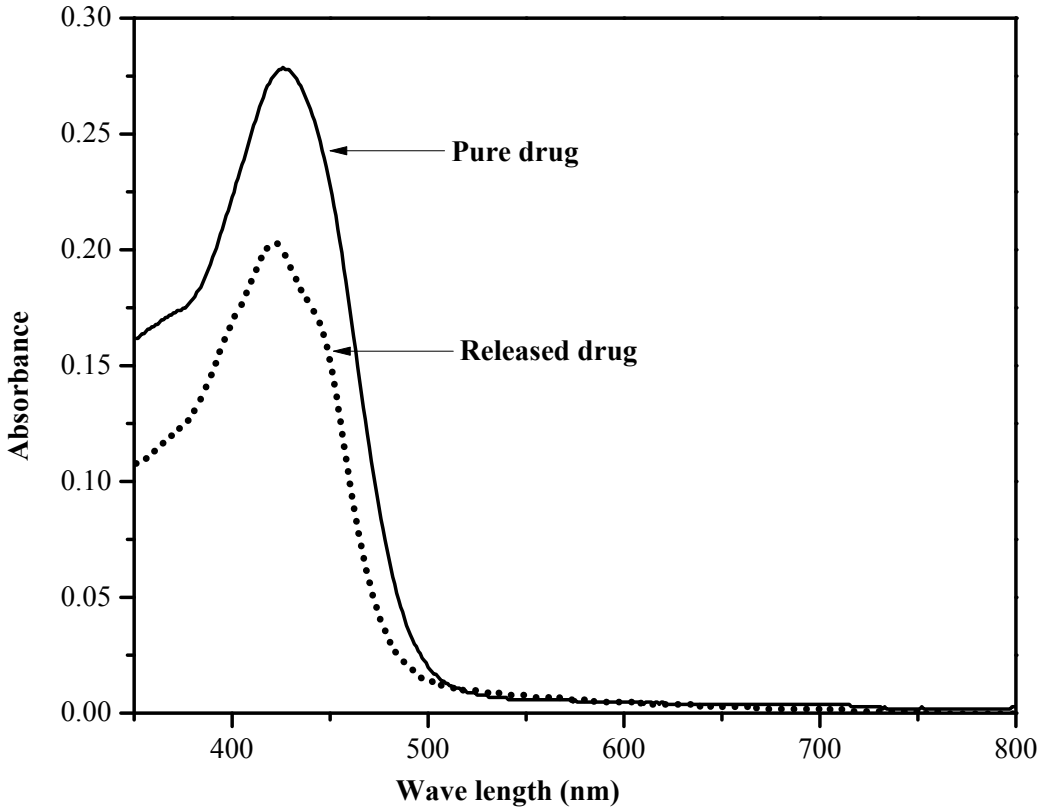

Fig. 10. UV-visible spectra of (a) pure drug and (b) released drug.

Table 1.

Composition of curcumin entrapped chitosan/nanocellulose/Tween 20 hydrogel formulations.

Formulation	Chitosan (w/v)%	Nanocellulose (w/v)%	Tween 20 (w/v)%	Glutaraldehyde (v/v)%	Curcumin (mg per 2.5 g of hydrogel disc)
CH/CNC/ TW-0%	2	0.5	0	0.2	1.5
CH/CNC/ TW-5%	2	0.5	5	0.2	1.5
CH/CNC/ TW-10%	2	0.5	10	0.2	1.5
CH/CNC/ TW-15%	2	0.5	15	0.2	1.5
CH/CNC/ TW-20%	2	0.5	20	0.2	1.5
CH/CNC/ TW-25%	2	0.5	25	0.2	1.5
CH/CNC/ TW-30%	2	0.5	30	0.2	1.5